Robust feedback control for automated force/position control of piezoelectric tube based microgripper

Mounir Hammouche, Philippe Lutz, *Member, IEEE,* and Micky Rakotondrabe, *Member, IEEE*

***Abstract*—This paper addresses the problem of automated grasping tasks using a piezoelectric microgripper, based on two piezoelectric tube actuators, for an accurate and rapid micro/nano manipulations. For this matter, we propose a strategy to control the position of one actuator and a hybrid approach that switches between force and position control of the second actuator. However, the nonlinearities and the uncertainties that characterize the piezoelectric actuators and the different properties of the manipulated objects make the control of such system not a trivial task. To handle this problem we propose to model the microgripper system by linear interval system, that embraces the parameters uncertainties, and synthesize a robust controller to control the interval system based on the classical output-feedback control design. The robust control synthesis consists on the search of robust gains for the controller that ensure the inclusion of the eigenvalues of the interval closed-loop system in a desired region of the complex plane. The effectiveness of the control strategy is illustrated by a real experimentation where the position and the manipulation force control show to maintain the desired performances under system uncertainties.**

***Index Terms*—Robust output-feedback, Interval models, SIVIA (Set Inversion via Interval Analysis), Microgripper, Automated pick-and-place, Force/Position control, Piezoelectric actuator.**

I. Introduction

THE use of piezoelectric actuators in the conception of micro/nano-manipulation systems has been generating considerable interest in the last years due to their high speed (large bandwidth up to 1kHz), high precision (sub-nanometric), high resolution, and multi-degrees of freedom possibility [1], [2], [3], [4]. Recently, the micro-robotic community has taken interest in developing microgrippers systems based on two collaborative piezoelectric actuators with cantilevered structure that allow scientists and engineers to systematically perform micro/nano manipulations such as pick-and-place tasks. Several prototypes of microgrippers have been developed to manipulate micro/nano objects with different shapes and characteristics [1], [3], [5], [6]. However, the control of piezoelectric microgrippers highlight the difficulty in attaining the desired operation efficiency due to the actuators nonlinearities (hysteresis, time varying parameters, creep, etc), the sensitivity to the ambient conditions and the lack of adequate sensors in micro-world. The former characteristics impact considerably the approximated model of the actuators and induce a change in their resonant frequencies. Furthermore, in micro/nano manipulation, the manipulated objects are usually so fragile and if the desired performance (overshoot and rapidity) are not well respected under the above mentioned factors, the manipulated object may be damaged. Actually these factors must be taken into account by including enough robustness to the controller otherwise they may lead to degradation of the closed-loop performance or the instability of the overall system.

For the success of micro-objects manipulation, in addition to the necessity of the robust controllers, the manipulation process should be automated with less human intervention to guarantees repeatable, stable and accurate micro/nano manipulation tasks. Indeed, the automated control of these microgrippers are usually achieved by controlling on position one of the two cantilevers while controlling on force the second one to maintain the manipulated object and to avoid the deterioration of the object as well as the actuator [1], [2], [3]. However, the main problem of this control strategy is that the second actuator (the cantilever controlled on force) must be initially in contact with the manipulated object to prevent generating high control input when the object is not in contact. For this reason we propose, in this paper, to control the second cantilever both on position and on force and use a decision mechanism to switch between them when the actuator is in contact. Moreover, the control on position of the second actuator gives further possibility to apply the dynamical release strategy to perform an accurate releasing of the micro/nano object in the desired place in the presence of adhesion force between the cantilever and the micro/nano object [7]. The dynamical releasing strategy can be done by forcing both cantilevers of the microgripper to move simultaneously with high speed in the opposite direction of the micro/nano object.

Until now, some robust control schemes have been designed to make the piezoelectric microgrippers track automatically a certain trajectory for manipulation tasks [1], [5], [8], [9]. In [5], khadraoui et al propose an automated pick-and-place with interval-based controller design to control robustly the force and the position of the microgrippers based on the inclusion theorem [10]. Moreover, the interval-based controller design proposed by khadraoui et al consists on modeling the piezoelectric actuator by bounding the parameters uncertainties by intervals using a transfer function representation. However, the proposed interval-based approach with transfer function representation was not well adapted to multivariable systems. For that matter we focus our attention on the interval state-space

FEMTO-ST Institute,UMR CNRS 6174 - UBFC / ENSMM / UTBM Automatic Control and Micro-Mechatronic Systems depart., AS2M 24 rue Alain Savary,
25000 Besançon, France,
corresponding author: mounir.hammouche@femto-st.fr.

models using a regional pole assignment technique to provide a guaranteed stability margin and a desired performance with low-order controllers using the state/output-feedback design.

The robust controller synthesis for a class of interval systems with state-space representation has been considered in several works [11], [12]. Actually, the previous works are focused on placing the coefficients of the system's closed-loop characteristic polynomial within a desired closed-loop interval characteristic polynomial, which makes them manageable by manual calculation in the case of simple problems whilst the computational complexity grows quickly with the number of free design parameters and with the number of uncertain specifying parameters. Furthermore, only the degree of stability of the closed-loop system with state-feedback was addressed and no performances measure was discussed. As it is not always that all states of the system can be obtained, we restrict the analysis to robust output-feedback design which is not addressed in the previous works that deal with interval systems.

In this paper, the modeling, the robust force/position control design, and the automation of the grasping tasks of a microgripper, that consists of two piezoelectric tube actuators, are addressed. Foremost an interval approach is adopted to approximate the voltage-force/voltage-position models by interval state-space models that embrace the uncertainties of the actuators, the sensitivity to the ambient conditions, and the characteristics of the different manipulated objects. Furthermore, an algorithm based on Set Inversion Via Interval Analysis (SIVIA [13]) combined with interval eigenvalues computation is proposed to synthesis robust force and position controllers. Finally, an automated control strategy for pick-and-place tasks that uses the introduced robust feedback controllers design, and which also contains a decision mechanism to switch between the two force and positions controllers, is proposed and validated experimentally.

II. Interval analysis and matrix theory preliminaries

A real interval matrix is a matrix in which all the elements are interval numbers or belongs to a specified interval [14]. Furthermore, an interval matrix is also defined as a family of matrices:

$$\boldsymbol{A} := [\underline{A}, \overline{A}] = \left\{ A \in R^{n\times n};\, \underline{A} \leq A \leq \overline{A} \right\} \tag{1}$$

where $\underline{A}$, $\overline{A} \in R^{n\times n}$, $\underline{A} \leq \overline{A}$ being given matrices and the inequality being considered element-wise, i.e. $\underline{A}_{i,j} < \overline{A}_{i,j}$ for all $i,\ j$.

A. Eigenvalue computation

The eigenvalue set $\Lambda(\boldsymbol{A})$ corresponding to $\mathbf{A}$ is defined as the set of all eigenvalues overall $A \in \mathbf{A}$, that is [15],

$$\Lambda(\boldsymbol{A}) = \{\lambda + i\mu \mid \exists A \in \boldsymbol{A}, \exists x \neq 0 :\ Ax = (\lambda + i\mu)x)\} \tag{2}$$

Some interval matrices have symmetric interval matrices as subclass. In such a case, the symmetric interval matrix $\mathbf{A^S}$ corresponding to interval matrix $\mathbf{A}$ is defined as the family of all symmetric matrices denoted A^s in $\mathbf{A}$, that is,

$$\mathbf{A}^S = \left\{ A^S \in \mathbf{A} \right\} \tag{3}$$

It is worthy that a real symmetric interval matrix $\mathbf{A^S} \in IR^{n\times n}$ has n interval eigenvalues which are real.

The recent advances on interval analysis computation have provided a new opportunity to estimate the eigenvalues of interval matrices. For example, Deif [16] and Kolev [17] proposed their exact bounds under some hard assumptions [18]. A cheap formula (easily computed) for an enclosure is proposed by Rohn [19] for symmetric interval matrices class. Rohn's result was extended to generalized interval matrices by Hladík [18]. Hladík's formula gives a unique interval in which all eigenvalues are bounded. Furthermore, other interesting method for interval eigenvalues computation is the vertex approach [20], [21]. The later is based on the calculation of all exposed edges of interval matrix and the convex hull of all roots of possible characteristic equations.

III. Robust controller design using interval analysis

In this section we propose a robust output-feedback design for interval state-space systems with regional eigenvalues assignment technique that will be used later to control the piezoelectric actuator on position and on force.

A. Overview of interval output-feedback design

The robust output-feedback control problem is among the most important open questions in control engineering [22]. The objective of the robust output-feedback, in this work, is to find the feedback matrix gain K such that the closed-loop system meets some transient performances specifications under system uncertainties described by an interval system. In other word, the designed controllers are robust in the sense that all the eigenvalues of the interval closed-loop system are clustered inside a desired region of the complex plane.

Consider a linear Multi Input Multi Output interval uncertain system described by the following interval state-space equation:

$$\begin{cases} \dot{x}(t) = \boldsymbol{A}x(t) + \boldsymbol{B}u(t) \\ y(t) = \boldsymbol{C}x(t) \end{cases} ; \tag{4}$$

where $x \in R^n$, $u \in R^m$, $y \in R^p$, $\boldsymbol{A} \in IR^{n\times n}$, $\boldsymbol{B} \in IR^{n\times m}$, and $\boldsymbol{C} \in IR^{p\times n}$. The matrices $\boldsymbol{A}$, $\boldsymbol{B}$, $\boldsymbol{C}$ are unknown but bounded by elements lying in known upper and lower bound; i.e. $\boldsymbol{A} = [\underline{A}, \overline{A}]$, $\boldsymbol{B} = [\underline{B}, \overline{B}]$, and $\boldsymbol{C} = [\underline{C}, \overline{C}]$.

Let us assume that the pair $\boldsymbol{A}$, $\boldsymbol{B}$ of the model (4) is controllable in the sense of the definition of Smagina Y,2002 [11]. In simple output-feedback model, the linear output-feedback control law is presented by:

$$u(t) = Ky + Nr(t). \tag{5}$$

where K is the output-feedback gain, N is the feedforward control gain, and $r(t)$ is the reference input.

In order to eliminate any steady-state offset that may occur, a compensator must be added to the closed-loop system. The static feedforward gain (DC-gain) N is not the ideal solution in the case of interval system because it always creates a non-null steady-state error. For this purpose we propose to use the integral compensator. It always ensures a zero error tracking control. The proposed control law is therefore given by:

$$u(t) = k_y y + \xi(t) K_i \tag{6}$$

where $\xi(t)$ is the integral of tracking error (i.e. $\dot{\xi} = r(t) - y(t)$).

The output-feedback control law can be presented by $(n+1)$ dimensional augmented state vector formed by the state vector $x(t)$ and the integrator variable $\xi(t)$. The state equations for both $\dot{x}(t)$ and $\dot{\xi}$ are consequently:

$$\begin{cases} \dot{x}(t) = (\boldsymbol{A} + \boldsymbol{B} K_y \boldsymbol{C}) x(t) + \boldsymbol{B} K_i \xi(t) \\ y(t) = \boldsymbol{C} x(t) \\ \dot{\xi}(t) = r(t) - y(t) = r(t) - \boldsymbol{C} x(t) \end{cases} \tag{7}$$

From (7), the augmented state-space model is yielded:

$$\begin{pmatrix} \dot{x}(t) \\ \dot{\xi}(t) \end{pmatrix} = \underbrace{\begin{pmatrix} (\boldsymbol{A} + \boldsymbol{B} K_y \boldsymbol{C}) & \boldsymbol{B} K_i \\ -C & 0 \end{pmatrix}}_{[\boldsymbol{A}_{aug\_cl}]} \begin{pmatrix} x(t) \\ \xi(t) \end{pmatrix} + \underbrace{\begin{pmatrix} 0 \\ 1 \end{pmatrix}}_{[\boldsymbol{B}_{aug\_cl}]} r(t)$$

$$y(t) = \underbrace{\begin{pmatrix} \boldsymbol{C} & 0 \end{pmatrix}}_{[\boldsymbol{C}_{aug\_cl}]} \begin{pmatrix} x(t) \\ \xi(t) \end{pmatrix} \tag{8}$$

B. Problem formulation using Set-Inversion

The problem of robust output-feedback control can be outlined by finding the gain matrix $[K]$ (with $[K] = [[K_y]\ [K_i]]$) that assigns the system eigenvalues to an arbitrary set taking into account the uncertainty of the interval system. That is, the problem consists in finding the interval parameters $[K]$ of the closed-loop system such that the inclusion eq.9 is satisfied.

$$eig\left[A_{aug\_cl}([A],[B],[C],[K])\right] \subseteq \Omega_{Desired\,region} \tag{9}$$

where A_{aug_cl} is the augmented closed-loop matrix of the system (8) and $\Omega_{Desired\,region}$ is the desired region for the interval eigenvalues situated in the left-half of the complex plane.

This problem can be converted into a set-inversion problem which can be solved easily using inversion algorithms. A set inversion operation consists to search the reciprocal image called subpaving of a compact set [14]. In our case in order to solve this set inversion problem, we propose to adapt the Set Inversion Via Interval analysis (SIVIA) algorithm, introduced by Jaulin in 1993 [13], that we will call the recursive SIVIA-based algorithm. In this recursive SIVIA-based algorithm, the aim is to approximate with subpaving the set solutions $[K]$ that satisfy the inclusion eq.9.

The recursive SIVIA-based algorithm to compute the output-feedback parameters is outlined in Table1. It requires initial box $[K_0]$ that may contain the solution, the interval state-space matrices, the desired region of eigenvalues, and the required accuracy for the paving ϵ. Since the closed-loop matrix is non-symmetric, the eigenvalues interval approximation are calculated by mean of Hladík formula or the vertex approach, whereas in the case of symmetric matrix Rohn's formula can be used [18], [19], [21]. The proposed algorithm provides complete information about the ranges of feedback gains including: inner (solution), outer (undefined), and unfeasible (no solution) subpavings where all the sets subpavings are initially empty. However, the robust gain matrix $K = [K_y\ K_i]$ (non-interval) can be chosen randomly from the set solution $[K]$ to be sure that this gains matrix will assign all the closed-loop system eigenvalues inside the desired region whatever the system matrices $(A,\ B,\ C)$ are inside the interval system $(\boldsymbol{A},\ \boldsymbol{B},\ \boldsymbol{C})$.

TABLE I
THE PROPOSED RECURSIVE SIVIA-BASED ALGORITHM.

	SIVIA(in: $[A],[B],[C],[K] = [intialbox], [k_{in}] = \oslash, [K_{out}] = \oslash, [K_{Unfeasibl}] = \oslash, \epsilon, Y = \Omega_{Desiredragion}$)
Step 1	Iteration i - Calculate $A_{aug\_cl}([A],[B],[C],[K])$ - Calculate $eig([A_{aug\_cl}])$
Step 2	-If $eig([A_{aug\_cl}]) \subseteq Y$ Then $[k_{in}] = [k_{in}] \cup [K]$ Go to step 6
Step 3	-If $eig([A_{aug\_cl}]) \cap Y = \oslash$ Then $[k_{Unf}] = [k_{Unf}] \cup [K]$ Go to step 6
Step 4	-If $[K] < \epsilon$ Then $[k_{out}] = [k_{out}] \cup [K]$ Go to step 6
Step 5	- Else bisect $[K]$ and stack the two resulting boxes.
Step 6	-If the stack is not empty, then unstack into $[K](i+1)$, increment i and go to Step 1. -Else End.

IV. MODELING OF PIEZOELECTRIC TUBE ACTUATOR

During the experimental process we focus on the control of the manipulation force only on one axis (one degrees of freedom: 1-DoF). We will note U_x the related applied voltage, σ_x and F_m are the resulting deflection and the applied force to the manipulated micro-object respectively in the x direction. In order to inflect the tube along X-axis , we apply a voltage on one electrode and an inverse sign voltage with the same amplitude on the other electrode in the opposite side. In the terminal of the piezoelectric tube, we have placed a small cube with perpendicular and flat sides to be able to measure the linear displacement of the tube deflections as depicted in fig.1.

The relation between the U_x, σ_x and F_m can be expressed by the following linear equation (10), whereas the actuator nonlinearities, sensitivity to the ambient conditions as well as the characteristics of the manipulated object will be approximated later by parametric uncertainties bounded by intervals [1].

$$\sigma_x = (d_p U_x - s_p . F_m) . \Upsilon(s) \tag{10}$$

where s_p and d_p are the compliance of the actuator and the piezoelectric constant, $\Upsilon(s)$ represents the dynamic part of the actuator (with $\Upsilon(0) = 1$).

The compliance s_p of the actuator is identified experimentally by applying a known constant force F by pushing the force sensor toward the piezotube actuator along the x-axis using a manual precise positioning table. Then, the compliance of the actuator is calculated from the resulting deflection as follow: $s_p = \frac{\sigma_x}{F}$ [1].

The dynamic of the manipulated micro-object can be represented by a second order model of spring-mass-damper system, as shown in fig.1. And it can be expressed by the following equation (11):

$$\sigma_x - \sigma_{nc} = s_0.F_m.\Psi(s) \tag{11}$$

where $s_0 = \frac{1}{k_e}$ represents the micro-object compliance and $\Psi(s)$ is the dynamic part.

After replacing the deflection in (10) by that of (11), we deduce the expression of the manipulation force:

$$F_m = \frac{d_p.\Upsilon(s).U_x}{s_0.\Psi(s) + s_p.\Upsilon(s)} + \frac{\sigma_{nc}}{s_0.\Psi(s) + s_p.\Upsilon(s)} \tag{12}$$

Finally, to obtain the interval model of the piezoelectric actuator that includes the nonlinearities and uncertainties of the piezoelectric tube actuator, we describe each parameter of $\Upsilon(s)$ by intervals $[\Upsilon(s)]$. In micro/nano manipulation, the control performances are affected by the manipulated objects which result in a significant change in the behavior of the actuator. However, it is not practical to identify the model and to design the controller at each change of the manipulated object. For this matter, we propose to use intervals to model and to bound the compliance of the manipulated objects. Thus: $[s_0] = [s_0^-, s_0^+]$ Where s_0^- represents the compliance of the most rigid object while s_0^+ refers to the most flexible object. Furthermore, the dynamic of the manipulated object is supposed to be quasi-static (i.e. $\Psi(s) = 1$) and its effects are considered as system uncertainties and are supposed to be belong the different sources of uncertainties interval model of the actuator $[\Upsilon(s)]$. This hypothesis will be verified in the experimental results. Additionally, the compliance of the actuator s_p and the piezoelectric constant d_p can be considered as interval parameters. Finally, we get the following interval model:

$$[F_m] = \frac{[d_p].[\Upsilon(s)].U_x}{[s_0] + [s_p].[\Upsilon(s)]} + \frac{\sigma_{nc}}{[s_0] + [s_p].[\Upsilon(s)]} \tag{13}$$

In this experimental case, the compliance of the elastic object and the the most rigid object are shown to be belong the following interval: $[s_o] = [1.93, 3.738]\mu m/mN$ [5].

In the later sections of this paper we will use a decision mechanism to switch between the control on position into the control on force when the micro object is in contact with the actuator. Hereby, the actuator will be initially in contact with the micro object when the decision mechanism switches to the control on force (i.e. $\sigma_{nc} = 0$). Consequently, we have the following linear transfer voltage-force when the contact is established which is taken from eq.13:

$$[G_{UF}] = \frac{F_m}{U_x} = \frac{[d_p].[\Upsilon(s)]}{[s_0] + [s_p].[\Upsilon(s)]} \tag{14}$$

Notwithstanding, when the actuator is controlled on position only when the micro object is not in contact (i.e. $F_m \simeq 0$), the linear transfer function that links the input U_x and the output σ_x (voltage-deflection) can be derived easily from eq.10:

$$[G_{U\sigma}] = \frac{\sigma_x}{U_x} = [d_p][\Upsilon(s)] \tag{15}$$

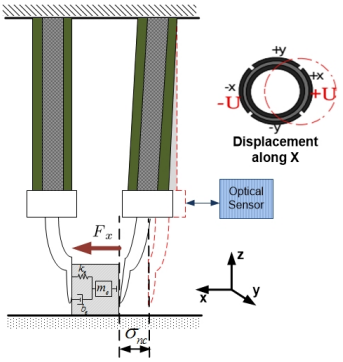

Fig. 1. Structure and operation of the piezoelectric microgripper based on two piezoelectric tube actuators.

V. Automated control structure

In the previous works that dealt with automated microgripper, one cantilever actuator is controlled on force while the other is controlled on position in order to perform one axis (1-dof) manipulation tasks. In this paper we keep the same idea however to make the pick-and-place task fully automated with less human intervention, we propose a new strategy based on controlling the second cantilever both on position and on force and use a decision mechanism to automatically switch between them. The main focus here is to control the piezotube actuator with a robust deflection technique to approach the micro-object. Then once the actuator is in contact with the micro-object the decision mechanism automatically switches the control on force. The decision mechanism is taken based on the estimated value of the manipulation force with the help of a predefined threshold calculated experimentally. Primary the decision mechanism is considered as a predefined threshold decision-making, however, in the upcoming work we will focus on using an intelligent method to combine the force/position controller with a self-adaptive threshold. The overall structure of the proposed automated control strategy is depicted in fig.2. Each block will be detailed in the next subsections.

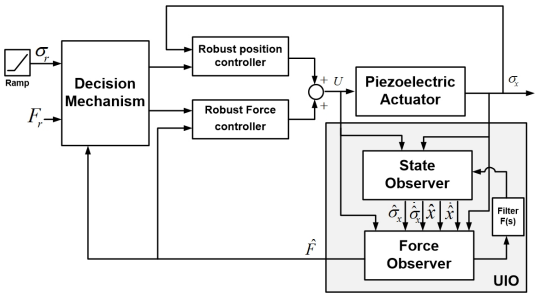

Fig. 2. Overall structure of the proposed automated control strategy.

A. Design of position controller

In this subsection, we will employ the robust output-feedback design and the interval model of the microgripper system to find the robust feedback gains that permit to control the piezoelectric microgripper on position with maintaining

the desired performance under system uncertainties. Therefore, the interval voltage-deflection model proposed in the previous section will be used. Foremost, to characterize the dynamics $G_{U\sigma}$ parameters, we apply a step voltage U_x of amplitude 200V and capture its corresponding σ_x deflection. To identify the dynamic part $G_{U\sigma}$ of the actuator, we use System Identification MatlabToolbox. Particularly, a second order model has been chosen because it is largely sufficient to represent the dynamics of the piezoelectric tube.

Finally, to obtain the interval model of the piezoelectric actuator that includes the nonlinearities and uncertainties of the piezoelectric actuator as explained previously, we propose to consider each parameter of dynamics $\Upsilon(s)$ as center and adding a radius of 10% in order to have an interval parameter. These 10% are a good compromise between finding a width of uncertainty as large as possible and the possibility to have a solution of the feedback controller [5]. We therefore obtain:

$$[G_{U\sigma}](s) = \frac{[b_0]\, s^2 + [b_1]\, s + [b_2]}{s^2 + [a_1]\, s + [a_2]} \tag{16}$$

where

$$\begin{array}{ll} [b_0] = 0; & [a_1] = [3.6033, 4.4041] * 1.0e+07; \\ [b_1] = [4.1424, 5.0630] * 1.0e+09; & [a_2] = [1.6147, 1.9735] * 1.0e+10; \\ [b_2] = [1.4045, 1.7166] * 1.0e+13; & \end{array}$$

The above interval transfer function model of the piezoelectric tube actuator can be expressed by the flowing state-space model in control canonical form:

$$\begin{cases} \dot{x}(t) = \boldsymbol{A}x(t) + \boldsymbol{B}u(t) \\ y(t) = \boldsymbol{C}x(t) + \boldsymbol{D}u(t) \end{cases} \tag{17}$$

$$\boldsymbol{A} = \begin{bmatrix} 0 & 1 \\ -[a_2] & -[a_1] \end{bmatrix};\ \boldsymbol{B} = \begin{bmatrix} 0 \\ 1 \end{bmatrix};\ \boldsymbol{D} = [b_0]$$

$$\boldsymbol{C} = \begin{bmatrix} [b_2] - [a_2][b_0] & [b_1] - [a_1][b_0] \end{bmatrix}$$

The use of the interval model of the piezoelectric tube allows us to find a robust output-feedback controller which satisfies the desired performances with the help of recursive SIVIA-besed algorithm described in Table.1. Indeed, in micro/nano manipulation and assembly applications, rapidity is highly required and overshoot is extremely undesirable because it may cause micro/nano objects damage. Therefore, the following desired performances are adopted: negligible overshoot (1%) and a settling time $T_s \leq 40ms$, which corresponds to $\xi_1 = \eta.\omega_n = 74.9$, where η and ω_n are the damping ratio and natural frequency respectively.

To find the set solution of the robust gain matrix $[K]$ (with $[K] = [[K_y]\ [K_i]]$), we employ the recursive SIVIA-based algorithm (Table.1). We select an initial box $[K_y] \times [K_i] = [-5 \times 10^1, 5 \times 10^1] \times [-1{\times}10^3, 1{\times}10^3]$ and an accuracy of paving $\epsilon = 0.1$. The obtained results are depicted in fig.3. The red boxes refer to the inner subpavings $[K_{in}]$ (the set solutions $[K_y]$ and $[K_i]$ that satisfy the inclusion eq.9). The white boxes refer to the set of gain matrix $[K_{Unfeasible}]$ where the inclusion condition (eq.9) is not satisfied. The yellow boxes corresponds to $[K_{out}]$ where no decision on the inclusion (eq.9) is taken.

Furthermore to test the obtained solutions we arbitrarily select the controller parameters $K_y = -1$ and $K_i = 700$

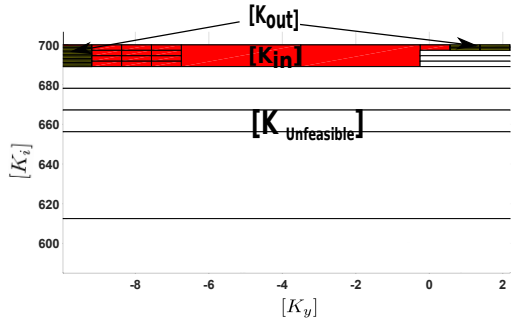

Fig. 3. Resulting subpaving $[K_y]$ and $[K_i]$ with : red (solution boxes), white (no solution), yellow (no decision).

from the solution boxes fig.3. The simulation of the closed-loop system step response is depicted in fig.4. In the figure, three simulation results are performed using three different values of the system matrices (A, B, C) inside the interval system$([A], [B], [C])$, where the sup(), inf(), and mid() refer to the superior, inferior, and middle values of the interval matrices. Actually it can be seen clearly that all of the step responses of the closed-loop system satisfy the desire performance with negligible overshoot (1%) and with a settling time $T_s \leq 40ms$.

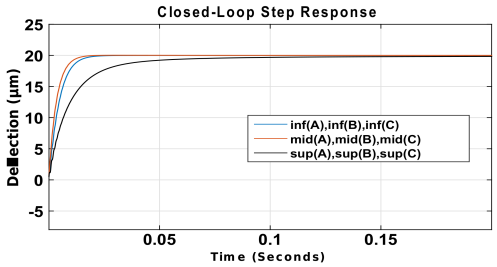

Fig. 4. Step response of the voltage-deflection system (Simulation using Matlab).

B. Design of force controller

In the force control design, we have used the robust output-feedback design exactly in the same way than the previous subsection of position controller design with employing the voltage-force interval model $[G_{UF}]$. However, due to the lack of a convenient and integrable force sensor in micro-nano world, we propose to use the Unknown Input Observer (UIO), introduced by the authors in [23], to estimate the manipulated force. The observer is based on considering the force as an unknown input disturbance and estimating this latter by the inverse dynamics. The convergence and the performance of the estimated force has already been illustrated and a set of experimental results have confirmed the efficiency of the observer [23]. The inputs of the observer are the input voltage U_x and the measured deflection σ_x, as depicted in fig.2.

The obtained set solutions that correspond to the parameters $[K_y] \times [K_i]$ are shown in fig.5. We select arbitrary from the solution boxes fig.5 the controller parameters $K_y = -0.1 \times 10^{-3}$ and $K_i = 0.3$.

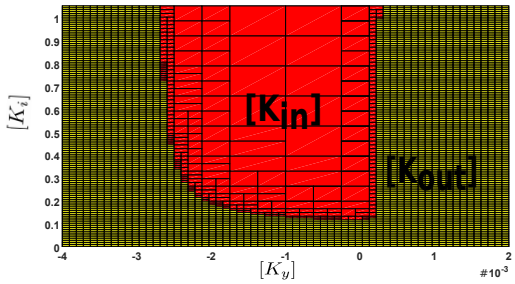

Fig. 5. Resulting subpaving of $[K_y]$and $[K_i]$ with : red (solution boxes), yellow (no decision).

The simulated step response for the closed-loop system using three different values of the system matrices (A, B, C) inside the interval system$([A], [B], [C])$ are depicted in fig.6. As noticed previously all of the step responses of the closed-loop system satisfy the desired performances with negligible overshoot (1%) and with a settling time $T_s \leq 20ms$.

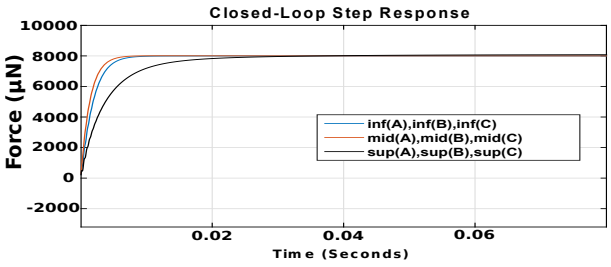

Fig. 6. Step response of the voltage-force system (Simulation using Matlab).

VI. Experiments

The previous section was devoted to design the robust output-feedback controllers as well as the UIO observer. However, only the robust gains of the output feedback controllers for both force and position are calculated and tested in simulation and the observer was not. In this section, the designed controllers and the UIO observer are implemented separately and tested experimentally, then the proposed automated robust force/position control structure is implemented and validated experimentally.

The experimental setup is represented in fig.7. It is composed of a piezoelectric tube actuator (PT230.94), an optical displacement sensors (LC2420 from Keyence company), a voltage amplifier (up to $\pm 200V$), a force sensor from femtotools-company (FT-S10000) and a computer with Matlab/Simulink software. The piezoelectric tube is made of lead-zirconate-titanate (PZT) material coated by one inner electrode (in silver) that serves as ground and four external electrodes (in copper-nickel alloy) for the electrical potentials with a size of 30 mm × 3.2 mm × 2.2 mm (Length × outer dimension × inner dimension). The actuator and the sensors are connected to the computer through a dSPACE-1103 board. In addition in order to regulate the ambient temperature, we use a resistance heating wire around the piezoelectric actuator as shown in the fig.7 and a precision reference thermometer (Eurolec RT161). Fuerthermore, a micro scale camera (DigMicro) was used to visualize the deflection of the piezoelectric tube.

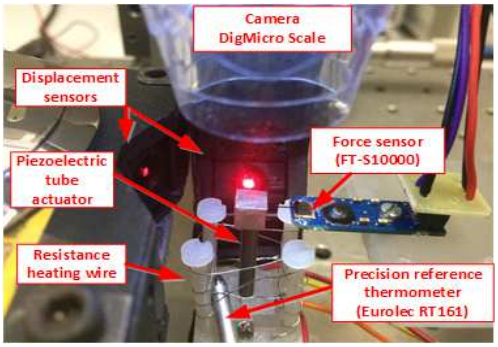

Fig. 7. Presentation of the experimental setup.

A. Validation of the position control

The goal of this subsection is to validate experimentally the control on position of the piezoelectric tube actuator using the robust output-feedback design. Fig.8 represents the experimental results of the voltage-deflection closed-loop response. The goal of the experimental results is to to demonstrate that the closed-loop system satisfies the desired performance under the actuator nonlinearities and its sensitivity to the ambient conditions.

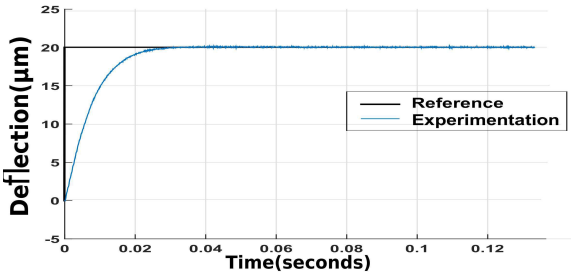

Fig. 8. Step response of the position control system (experimental test).

B. Validation of the force control

The goal of this subsection is to validate experimentally the control on force of the piezoelectric tube actuator using the robust output-feedback design. Actually, in order to validate the proposed control schema, instead of manipulating a micro-object, we manipulate the cantilever of the force sensor as shown in fig.7. Fig.9 represents the experimental results of the voltage-force closed-loop response. However the results demonstrate that the closed-loop system satisfies the desired performance under system uncertainties.

C. COMPLETE AUTOMATED TASK

The objective if this subsection is to verify the effectiveness of the control strategy to achieve the automated pick-and-place task using a piezoelectric tube actuator. The experimental results are presented in Fig.10. This figure demonstrates that the overall structure of the proposed automated control

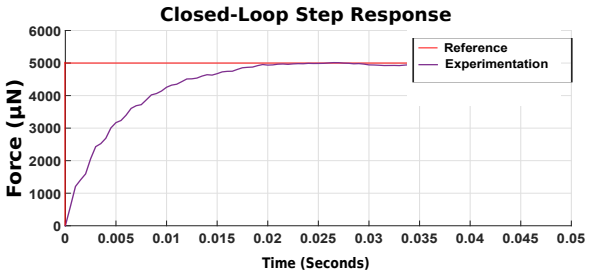

Fig. 9. Step response of the force control system (experimental test).

strategy has been successfully performed. Indeed, we can see clearly that the piezotube actuator is controlled on position to approach the object, and once the actuator is in contact with the object the decision mechanism automatically switches to control on force. Furthermore, the robustness of the outputs-feedback control has also been demonstrated though experiments that consist in maintaining the desired performance under system uncertainties and under external disturbances.

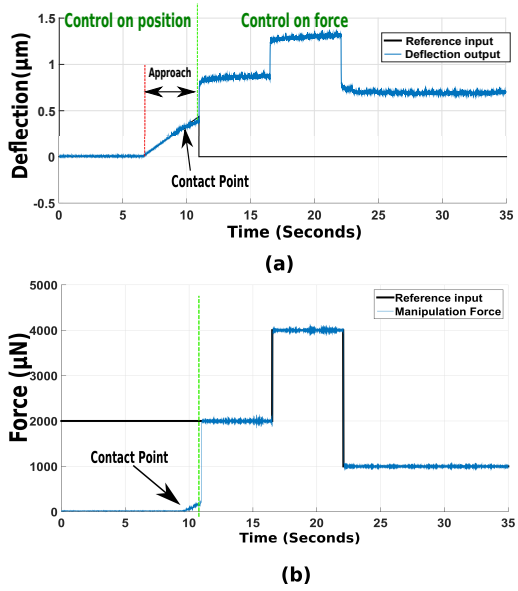

Fig. 10. Experimental results of an automated pick task demonstrates the switch between control on position into control on force.

VII. Conclusions

In this paper, interval modeling, robust control and automation of a piezoelectric microgripper based on two piezoelectric tube actuators are investigated. Indeed, a simple algorithm to synthesize the robust force/position controllers, with a classical output-feedback design, to control the piezoelectric microgripper under system uncertainties is introduced. The algorithm, called recursive SIVIA-based algorithm, is based on interval eigenvalue computations and set inversion techniques. Simulation validation and experimental applications were carried out to control on force and on position a piezoelectric tube actuator working in SISO (Single Input Single output) case which demonstrated the efficiency of the proposed control strategy. Furthermore, a hybrid control structure is proposed and validated experimentally for an automated grasping task. These results are promising for multi-axes micro/nano applications.

References

[1] M. Rakotondrabe, *Smart Materials Based Actuators at the Micro/Nano-Scale. Characterization, Control and Applications.* SPRINGER - VERLAG, Jan. 2013.

[2] H. Xie, M. Rakotondrabe, and S. Régnier, "Characterizing piezoscanner hysteresis and creep using optical levers and a reference nanopositioning stage," *Review of Scientific Instruments*, vol. 80, no. 4, p. 046102, 2009.

[3] S. Devasia, E. Eleftheriou, and S. O. R. Moheimani, "A survey of control issues in nanopositioning," *IEEE Transactions on Control Systems Technology*, vol. 15, no. 5, pp. 802–823, Sept 2007.

[4] J. Agnus, N. Chaillet, C. Clévy, S. Dembélé, M. Gauthier, Y. Haddab, G. Laurent, P. Lutz, N. Piat, K. Rabenorosoa *et al.*, "Robotic microassembly and micromanipulation at femto-st," *Journal of Micro-Bio Robotics*, vol. 8, no. 2, pp. 91–106, 2013.

[5] S. Khadraoui, M. Rakotondrabe, and P. Lutz, "Interval force/position modeling and control of a microgripper composed of two collaborative piezoelectric actuators and its automation," *International Journal of Control, Automation and Systems*, vol. 12, no. 2, pp. 358–371, 2014.

[6] B. Komati, C. Clévy, M. Rakotondrabe, and P. Lutz, "Dynamic force/position modeling of a one-dof smart piezoelectric micro-finger with sensorized end-effector," in *IEEE/ASME Advanced Intelligent Mechatronics (AIM),*. IEEE, 2014, pp. 1474–1479.

[7] D. S. Haliyo, S. Régnier, and P. Bidaud, "Manipulation of micro-objects using adhesion forces and dynamical effects," in *Experimental Robotics VIII*. Springer, 2003, pp. 382–391.

[8] M. Rakotondrabe, C. Clévy, and P. Lutz, "Modelling and robust position/force control of a piezoelectric microgripper," in *Automation Science and Engineering, 2007. CASE 2007. IEEE International Conference on*. IEEE, 2007, pp. 39–44.

[9] M. Rakotondrabe and I. A. Ivan, "Development and force/position control of a new hybrid thermo-piezoelectric microgripper dedicated to micromanipulation tasks," *IEEE Transactions on Automation Science and Engineering*, vol. 8, no. 4, pp. 824–834, 2011.

[10] M. Rakotondrabe, "Performances inclusion for stable interval systems," in *American Control Conference (ACC), 2011*. IEEE, 2011, pp. 4367–4372.

[11] Y. Smagina and I. Brewer, "Using interval arithmetic for robust state feedback design," *Systems and Control Letters*, vol. 46, no. 3, pp. 187 – 194, 2002.

[12] M. L. Prado, A. D. Lordelo, and P. A. Ferreira, "Robust pole assignment by state feedback control using interval analysis," in *World Congress*, vol. 16, no. 1, 2005, pp. 951–951.

[13] L. Jaulin and E. Walter, "Set inversion via interval analysis for nonlinear bounded-error estimation," *Automatica*, vol. 29, pp. 1053–1064, 1993.

[14] L. Jaulin, *Applied interval analysis: with examples in parameter and state estimation, robust control and robotics*. Springer Science & Business Media, 2001, vol. 1.

[15] B. M. Patre and P. J. Deore, "Robust state feedback for interval systems: An interval analysis approach." *Reliable Computing*, vol. 14, no. 1, pp. 46–60, 2010.

[16] A. Deif, "The interval eigenvalue problem," *ZAMM-Journal of Applied Mathematics and Mechanics/Zeitschrift für Angewandte Mathematik und Mechanik*, vol. 71, no. 1, pp. 61–64, 1991.

[17] L. Kolev and S. Petrakieva, "Assessing the stability of linear time-invariant continuous interval dynamic systems," *Automatic Control, IEEE Transactions on*, vol. 50, no. 3, pp. 393–397, 2005.

[18] M. Hladík, "Bounds on eigenvalues of real and complex interval matrices," *Applied Mathematics and Computation*, vol. 219, no. 10, pp. 5584–5591, 2013.

[19] J. Rohn, "A handbook of results on interval linear problems," *Internet text available at http://www. cs. cas. cz/rohn/handbook*, 2005.

[20] S. Bhattacharyya, H. Chapellat, and L. Keel, "Robust control: the parametric approach," *Upper Saddle River*, 1995.

[21] M. T. Hussein, "Assessing 3-d uncertain system stability by using matlab convex hull functions," *International Journal of Advanced Computer Science and Applications,(IJACSA)*, vol. 2, no. 6, 2011.

[22] V. L. Syrmos, C. T. Abdallah, P. Dorato, and K. Grigoriadis, "Static output feedback a survey," *Automatica*, vol. 33, pp. 125–137, 1997.

[23] M. Rakotondrabe and P. Lutz, "Force estimation in a piezoelectric cantilever using the inverse-dynamics-based uio technique," in *Robotics and Automation, 2009. ICRA'09. IEEE International Conference on*. IEEE, 2009, pp. 2205–2210.